Extremely Low Operating Voltage Green Phosphorescent Organic Light-Emitting Devices

Hisahiro Sasabe, Hiromi Nakanishi, Yuichiro Watanabe, Shogo Yano, Masakatsu Hirasawa, Yong-Jin Pu, and Junji Kido**

Organic light-emitting devices (OLEDs) are expected to be adopted as the next generation of general lighting because they are more efficient than fluorescent tubes and are mercury-free. The theoretical limit of operating voltage is generally believed to be equal to the energy gap, which corresponds to the energy difference between the highest occupied molecular orbital (HOMO) and the lowest unoccupied molecular orbital (LUMO) for the emitter molecule divided by the electron charge (*e*). Here, green OLEDs operating below a theoretical limit of the energy gap (E_g) voltage with high external quantum efficiency over 20% are demonstrated using *fac*-tris(2-phenylpyridine)iridium(III) with a peak emission wavelength of 523 nm, which is equivalent to a photon energy of 2.38 eV. An optimized OLED operates clearly below the theoretical limit of the E_g voltage at 2.38 V showing 100 cd m^{-2} at 2.25 V and 5000 cd m^{-2} at 2.95 V without any light outcoupling enhancement techniques.

1. Introduction

The panel efficiency of white organic light-emitting devices (OLEDs)[1–5] has just reached 90 lm W^{-1} at 1000 cd m^{-2} above the performance of a fluorescent tube.[6,7] Although OLED panels show superior performance, there is still much room (nearly 160 lm W^{-1}) for improvement, compared to the theoretical limit[8,9] of 248 lm W^{-1}. To meet this goal, OLEDs should achieve both high internal quantum efficiency and low operation voltage at the same time. So far, the internal quantum efficiency has reached almost unity by using a phosphorescent emitter and related materials;[10] therefore, a key issue is the reduction in operating voltage.

The limit of operating voltage is generally believed to be equal to the energy gap (E_g), which corresponds to the energy difference between the highest occupied molecular orbital (HOMO) and the lowest unoccupied molecular orbital (LUMO) for the emitter molecule divided by the electron charge (*e*). In fact, operating voltage is generally much higher or close to the E_g divided by *e* even in state-of-the-art OLEDs.[2–6] However, there are a few exceptions operating at half the E_g voltage.[11–13] Pandey has reported rubrene-based OLEDs with extremely low drive voltages of 1.1 V for 100 cd m^{-2} and 2.1 V for 1000 cd m^{-2}. The E_g of rubrene is 2.2 eV, so in their device, electroluminescence (EL) would be achieved with an Auger-assisted mechanism using multiple electrons for one photon.[12] In principle, EL based on this mechanism should use multiple electrons to generate one photon, thus leading to very low external quantum efficiency (EQE) of up to 0.4%.[13] However, for energy-saving displays and/or general lighting applications, OLEDs should require high power efficiency without any loss in EQE.

From a theoretical perspective, Meerheim has predicted the thermodynamic limit of the operating voltage by the use of an equation based on black-body radiation;[14] for example, the thermodynamic limit of the operating voltage in a green OLED is evaluated to be 1.95 V at 100 cd m^{-2}. Compared to the lowest voltage of 2.40 V, which is nearly equal to the theoretical limit of E_g voltage, in a *fac*-tris(2-phenylpyridine)iridium(III) [Ir(ppy)$_3$]-based OLED, there is still a large difference of 0.45 V from the theoretical limit.[15]

In this report, we develop a green OLED operating at 0.13 V lower than the E_g voltage by using a novel combination of electron transport layer (ETL) and electron injection layer (EIL). We use a well-known phosphorescent green emitter, Ir(ppy)$_3$, 2-phenyl–4,6-bis(3,5-di-4-pyridylphenyl)primidine (B4PyPPM) for the ETL[16] and lithium 2-(2′,2″-bipyridine-6′-yl)phenolate (Libpp) for the EIL,[17] respectively. An optimized OLED showed extremely low driving voltages of 2.03, 2.25, 2.49, and 2.95 V at 1, 100, 1000, and 5000 cd m^{-2}, respectively, without any light outcoupling enhancement techniques. This device also shows a power efficiency of 128 lm W^{-1} (84 cd A^{-1}) and a high EQE of 24% at the same time. By further improving the materials used, we realize operating voltages of 1.97 and 2.22 V at 1 and 100 cd m^{-2}, respectively.

Dr. H. Sasabe, H. Nakanishi, Y. Watanabe
S. Yano, Dr. M. Hirasawa, Prof. J. Kido
Department of Organic Device Engineering
Yamagata University
4-3-16 Jonan, Yonezawa, Yamagata 992-8510, Japan
E-mail: h-sasabe@yz.yamagata-u.ac.jp;
kid@yz.yamagata-u.ac.jp
Dr. H. Sasabe, Dr. M. Hirasawa, Dr. Y.-J. Pu, Prof. J. Kido
Research Center for Organic Electronics (ROEL)
Yamagata University
4-3-16 Jonan, Yonezawa, Yamagata 992-8510, Japan

DOI: 10.1002/adfm.201301069

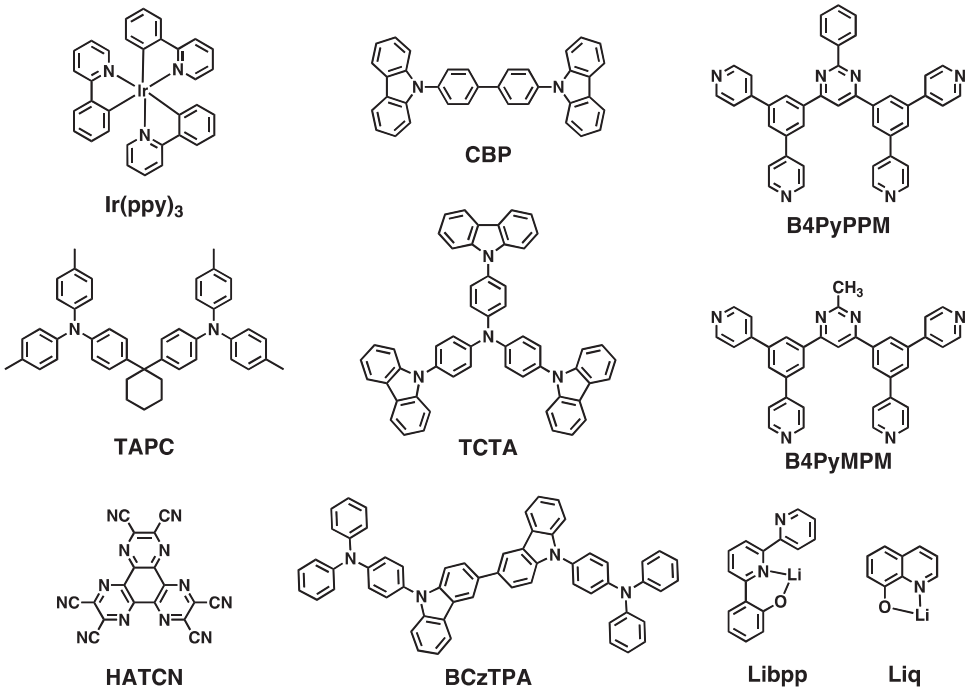

Figure 1. Chemical structures of materials used in this work.

2. Results and Discussion

2.1. OLED Structure

Unlike standard fluorescent OLEDs using singlet excitons, phosphorescent OLEDs use triplet excitons on the emitter. To maximize the phosphorescent OLED efficiency, the use of high triplet energy (E_T) materials is imperative to confine the triplet excitons on $Ir(ppy)_3$. We used 1,1-bis{4-[*N*,*N* -di(p-tolyl) amino]-phenyl}cyclohexane (TAPC) and B4PyPPM as the hole-transporting layer (HTL) and the ETL, respectively.[18] Because all the E_T values are reported to be larger than that of $Ir(ppy)_3$, the triplet exciton quenching of $Ir(ppy)_3$ at the emissive layer (EML)/HTL interface and/or the EML/ETL interface can be completely suppressed. For the hole-injection layer (HIL), we used 1,4,5,8,9,11-hexaazatriphenylene hexacarbonitrile (HATCN).[19] According to the report by Small and co-workers, the hole injection efficiency at the HATCN/arylamine interface reaches nearly 100%.[20] All the materials used in this work are shown in **Figure 1**.

2.2. Effect of Electron-Transporter and Electron-Injection Layer

One of the most effective ways to reduce the operating voltage is using a well-known technique of chemical doping of an alkaline metal, such as lithium or cesium, at the cathode interface.[21,22] Even with this method, however, the minimum operating voltage in a green OLED has been reported as 2.65 V at 100 cd m^{-2} in the literature,[23] so there is much room to reduce the operating voltage. As an alternative strategy, we have reported a new type of cathode interface layer composed of metal complexes.[24] These metal complexes can be evaporated at a relatively low temperature of 200–300 °C and are easy to handle under ambient conditions. Encouraged by these findings, we investigated several combinations of pyridine-containing ETLs and metal-complex-based EILs. Consequently, we found that a combination of B4PyPPM and the lithium complex Libpp gives superior current density–voltage (*J*–*V*) characteristics among 4,4′-*N*,*N*′-dicarbazolylbiphenyl (CBP)/$Ir(ppy)_3$-based standard OLEDs (**Figure 2**a). This combination can drastically reduce the operating voltage by 0.17 V at 100 cd m^{-2} and by 0.25 V at 1000 cd m^{-2} compared with those in the state-of-the-art green OLED[25] (Figure S1 and Table S1 in the Supporting Information).

2.3. Effect of Host Material

In general, phosphorescent OLEDs could introduce an intrinsic exchange energy loss derived from energy transfer, which is from the host's singlets to the guest's triplets. This energy transfer process significantly increases the operating voltage. In contrast, a direct recombination mechanism on the guest molecule can minimize the operating voltage because this mechanism does not include an energy transfer process.[26] From this perspective, we investigated OLEDs from the standpoint of the direct recombination mechanism to reduce the operating voltage, wherein 17 wt% $Ir(ppy)_3$-doped EML is used. Normally, the direct recombination mechanism occurs in a highly guest-doped EML (usually over 8 wt% in the $Ir(ppy)_3$ case; see also Figure S2 and Table S2 in the Supporting Information). As a host material, we used 3,3′-bicarbazole derivative (BCzTPA)[27] and 4,4,4-tris(*N*-carbazolyl)

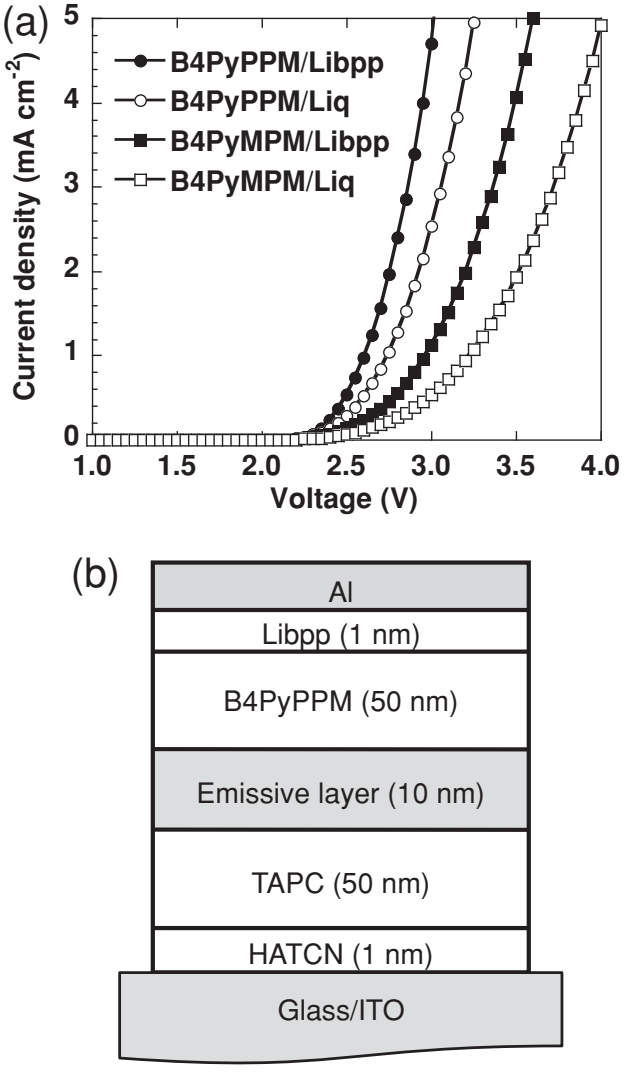

Figure 2. Device performances and structure of OLEDs: a) current density–voltage characteristics of devices with different ETL/EIL combination and b) standard structure of green OLEDs in this work.

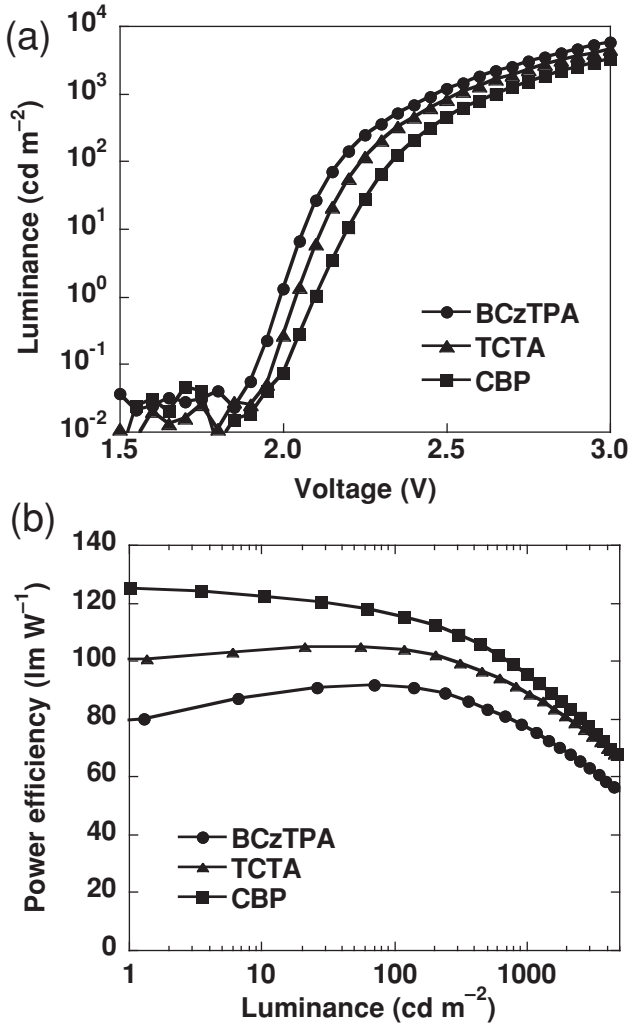

Figure 3. Effect of host material on device performances: a) luminance–voltage characteristics and b) power efficiency–luminance characteristics.

triphenylamine (TCTA) in addition to CBP. Furthermore, green OLEDs with a structure of [ITO (130 nm)/HATCN (1 nm)/TAPC (50 nm)/17 wt% Ir(ppy)$_3$-doped host (10 nm)/B4PyPPM (50 nm)/Libpp (1 nm)/Al (80 nm)] were fabricated to investigate the effect of host material (Figure 2b). The luminance–voltage (L–V) and power efficiency–luminance (PE–L) characteristics are shown in **Figure 3**. In these devices, host materials with shallower ionization potentials (I_p) give lower operating voltages (Figures S3 and S4A and Table S3 in the Supporting Information). Among these, a BCzTPA-based device showed lower operating voltage, the turn-on voltage at 1 cd m^{-2} was 1.99 V, and the applied voltages at 100 and 1000 cd m^{-2} were 2.17 and 2.47 V, respectively (Table S3, Supporting Information). These are the lowest operating voltages reported so far. Because this device gives a much lower operating voltage than the E_g voltage of 2.38 V, which is calculated by the peak EL emission wavelength of 523 nm, color changes in the EL spectra might be considered. However, we could not observe any change from EL spectra at 1, 10, and 100 cd m^{-2} (Figure S3B, Supporting Information). The angular dependence of luminous intensity can be fitted by the Lambertian distribution (Figure S4C, Supporting Information), so these performances are not overestimated.

2.4. Effect of a Double Emissive Layer

Although the BCzTPA-based device showed excellent low operating voltages, the EQEs are relatively low at ca. 18%. Therefore, we further improved the performance of the BCzTPA-based device by host engineering. Green OLEDs were fabricated with an emissive structure of [17 wt% Ir(ppy)$_3$-doped BCzTPA (5 nm)/Ir(ppy)$_3$-doped CBP (5 nm)], where the Ir(ppy)$_3$ concentration in the CBP layer was varied from 17 to 50 wt%. Among these devices, the 17 wt% Ir(ppy)$_3$-doped CBP device showed the highest efficiencies of 128 lm W^{-1} (84 cd A^{-1}) and 24% EQE with a turn-on voltage of 2.07 V (Table S5 in the Supporting Information). This OLED also showed low operating voltages

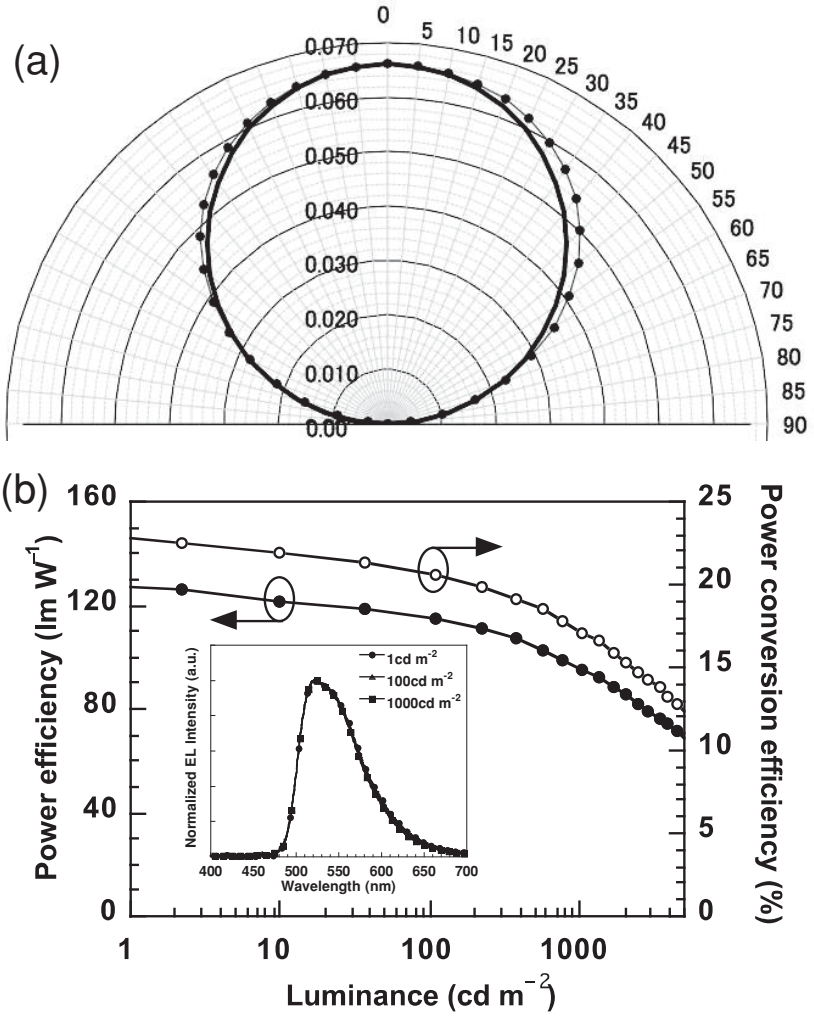

Figure 4. Device performances of the optimized OLEDs: a) the angular dependence of luminous intensity at 1000 cd m^{-2} and b) power efficiency–luminance–external power conversion efficiency characteristics. The inset shows EL spectra at 1, 100, and 1000 cd m^{-2}.

and high power efficiencies, 2.25 V/82.6 cd A^{-1}/115.6 lm W^{-1} at 100 cd m^{-2} and 2.49 V/76.3 cd A^{-1}/96.2 lm W^{-1} at 1000 cd m^{-2}. Surprisingly, even at 5000 cd m^{-2}, the operating voltage is 2.95 V. This is around five times higher luminance than that of the state-of-the-art green OLED at the same voltage.[5,23] The angular dependence of luminous intensity is almost fitted by the Lambertian distribution (Lambertian factor: 1.04; **Figure 4**a). The angular dependence is slightly asymmetric because of the slight misalignment of the attached device. By using the angular dependence of luminous intensity, we evaluated the power conversion efficiency (PCE), which is the ratio between the input of electrical power and the output. The external PCE–luminance characteristics are shown in Figure 4b. The 17 wt% $Ir(ppy)_3$-doped CBP device gave 23% external PCE at 1 cd m^{-2}. Assuming an outcoupling efficiency of 30% from the normal glass/ITO substrate, this external PCE equates to an internal PCE of 77%. In this device configuration, a higher $Ir(ppy)_3$ concentration in the CBP layer gives lower operating voltages (Figure S5, Supporting Information). Thus, the electron injection from ETL to EML is the voltage-determining step in this green OLED, which indicates that electrons are accumulated at the EML/ETL interface. The 50 wt% $Ir(ppy)_3$-doped CBP device showed the lowest operating voltages, 1.97 and 2.22 V at 1 and 100 cd m^{-2}, respectively (Table S5. Supporting Information).

2.5. Carrier Injection Process

To get a better understanding of the carrier injection process, we compared three types of devices with an EML structure: A) 17 wt% $Ir(ppy)_3$-doped BCzTPA (5 nm)/17 wt% $Ir(ppy)_3$-doped CBP (5 nm), B) BCzTPA (5 nm)/17 wt% $Ir(ppy)_3$-doped CBP (5 nm), and, C) 17 wt% $Ir(ppy)_3$-doped BCzTPA (5 nm)/CBP (5 nm). Compared with device A, device B with non-doped BCzTPA at the HTL interface showed almost the same current density, whereas device C with non-doped CBP at the ETL interface showed lower current density (Figure S6A in the Supporting Information). Device B gave an operating voltage of 2.27 V at 100 cd m^{-2}, which is comparable with the performance of device A. On the other hand, device C showed a higher operating voltage of 2.34 V (Table S6, Supporting Information). By combining these data and the aforementioned host comparison, it can be concluded that: i) better hole injection to EML can be realized by the use of BCzTPA owing to a favorable overlap of density-of-state distributions with HTL,[28] ii) $Ir(ppy)_3$ does not act as a hole-trapping site despite the difference in I_p levels between $Ir(ppy)_3$ and BCzTPA, iii) electron injection to EML is greatly enhanced by carrier trapping of $Ir(ppy)_3$, iv) electron injection from the ETL to CBP is difficult without doping of $Ir(ppy)_3$ on account of the shallow electron affinity level of CBP, and v) the emission zone is less than 5 nm from the EML/ETL interface because the performances of devices A and B are quite similar.

2.6. Device Operation Mechanism

An important question relates to how these OLEDs can operate at much lower voltages than the E_g voltage of 2.38 eV. Among inorganic LEDs, the presence of thermal energy allows inorganic LEDs to emit more optical power than they consume in electrical power. Santhanam and co-workers experimentally showed thermally pumped LEDs operating above unity efficiency.[29] Therefore, thermally assisted EL can be considered. Considering the aforementioned carrier injection process, we propose the following mechanism. i) A large amount of holes and electrons are blocked by the ETL and the EML owing to

large barriers and get accumulated at the EML/ETL interface. ii) As the holes get trapped on the $Ir(ppy)_3$ molecules, the LUMO of $Ir(ppy)_3$ is shifted to a deeper level by reduced electron–electron repulsion, and electrons become accessible from the ETL to the EML.[22] Thermally activated electrons following the Boltzmann distribution can be injected. iii) Finally, the holes and electrons are recombined and they emit light. A key factor in this system is carrier accumulation at the EML/ETL interface, in other words, the carrier blocking ability of the EML and ETL.[30] According to the Boltzmann distribution, the probability of electron injection to the energy barrier of 0.4 eV is very low, 1.7×10^{-7} at room temperature; thus, thermally activated holes should also be considered, and the probability of carrier injection to the energy barrier of 0.2 eV is 4.2×10^{-4}. Combining the photon number at 1 cd m^{-2} is ca. 10^{10} s^{-1} in a 2×2 mm^2 device and the radiative decay rate of $Ir(ppy)_3$ of ca. 10^6 s^{-1}, the required accumulated carrier number at the EML/ETL interface is evaluated to be ca. 10^9, which is equal to the accumulated carrier density of ca. 10^{10} cm^{-2}; this number is of same order as those reported in the literature.[31]

3. Conclusions

We have successfully demonstrated green OLEDs operating below a theoretical limit of operating voltage with high external quantum efficiency over 20% by using *fac*-tris(2-phenylpyridine) iridium(III) with a peak emission wavelength of 523 nm, which is equivalent to a photon energy of 2.38 eV. An optimized OLED operates clearly below the theoretical limit of 2.38 V showing 100 cd m^{-2} at 2.25 V and 5000 cd m^{-2} at 2.95 V without any light outcoupling enhancement techniques. Because the green OLEDs reported here do not use chemical doping, there is some room to reduce operating voltage. In addition, from this optimized device, one can optimistically expect 300 lm W^{-1} and 50% EQE at 100 cd m^{-2} from the use of light outcoupling enhancement techniques, such as a high-index substrate and a lens-based structure (2.5 times improvement).

4. Experimental Section

Materials: HATCN, CBP, TCTA, and Liq were purchased from eRay. TAPC was purchased from TCI. $Ir(ppy)_3$ was purchased from Chemipro Kasei. B4PyPPM,[16] B4PyMPM,[32] BCzTPA,[27] and Libpp[17] were synthesized according to procedures in the literature. All organic materials except HATCN and Liq were purified by temperature-gradient sublimation in vacuum.

Device Fabrication and Characterization: The substrates were cleaned with ultrapurified water and organic solvents, and then dry-cleaned for 30 min by exposure to UV–ozone. The organic layers were deposited onto the ITO substrate under the vacuum (ca. 10^{-5} Pa), successively. Liq and Al were patterned using a shadow mask with an array of 2 mm $\times$ 2 mm openings without breaking the vacuum (ca. 10^{-5} Pa). All devices were encapsulated immediately after preparation under a nitrogen atmosphere using epoxy glue and glass lids. The EL spectra were taken using an optical multichannel analyzer Hamamatsu Photonics PMA-11. The current density–voltage and luminance–voltage characteristics were measured using a Keithley source measure unit 2400 and a Minolta CS200 luminance meter, respectively. The angular dependence of luminous intensity was measured using a Keithley source measure unit 2400 and a Minolta CS2000. External quantum efficiencies were calculated from the front luminance, current density and EL spectrum. External power conversion efficiencies were calculated from the angular dependence of luminous intensity, current density, voltage, and EL spectrum. The ionization potential (I_p) was determined by an photoelectron yield spectroscopy (PYS)[33] under vacuum (ca. 10^{-3} Pa).

Supporting Information

Supporting Information is available from the Wiley Online Library or from the author.

Acknowledgements

The authors gratefully acknowledge the financial support in part by the New Energy and Industrial Technology Development Organization (NEDO) through the "Research and Development Program for Innovative Energy Efficiency Technology" and by KAKENHI (23750204).

Received: March 27, 2013
Revised: April 27, 2013
Published online: June 14, 2013

[1] J. Kido, M. Kimura, K. Nagai, *Science* **1995**, *267*, 1332.
[2] Y. Sun, N. C. Giebink, H. Kanno, B. Ma, M. E. Thompson, S. R. Forrest, *Nature* **2006**, *440*, 908.
[3] B. W. D'Andrade, J. Esler, C. Lin, V. Adamovich, S. Xia, M. S. Weaver, R. Kwong, J. J. Brown, *Proc. SPIE* **2008**, *7051*, 70510Q.
[4] S. Reineke, F. Lindner, G. Schwartz, N. Seidler, K. Walzer, B. Lussem, K. Leo, *Nature* **2009**, *459*, 234.
[5] a) M. G. Helander, Z. B. Wang, J. Qiu, M. T. Greiner, D. P. Puzzo, Z. W. Liu, Z. H. Lu, *Science* **2011**, *332*, 944; b) T.-H. Han, Y. Lee, M.-R. Choi, S.-H. Woo, S.-H. Bae, B. H. Hong, J.-H. Ahn, T.-W. Lee, *Nat. Photonics* **2012**, *6*, 105.
[6] T. Komoda, K. Yamae, V. Kittichungchit, H. Tsuji, N. Ide, *SID 12 Dig.* **2012**, 610.
[7] K. Sugi, T. Ono, D. Kato, T. Yonehara, T. Sawabe, S. Enomoto, I. Amemiya, *SID 12 Dig.* **2012**, 1548.
[8] Y. Ohno, *Opt. Eng.* **2005**, *44*, 111302.
[9] Y.-S. Tyan, *J. Photonics Energy* **2011**, *1*, 011009.
[10] C. Adachi, M. A. Baldo, M. E. Thompson, S. R. Forrest, *J. Appl. Phys.* **2001**, *90*, 5048.
[11] A. C. Morteani, A. S. Dhoot, J.-S. Kim, C. Silva, N. C. Greenham, C. Murphy, E. Moons, S. Ciná, J. H. Burroughes, R. H. Friend, *Adv. Mater.* **2003**, *15*, 1708.
[12] A. K. Pandey, J. M. Nunzi, *Adv. Mater.* **2007**, *19*, 3613.
[13] L. Qian, Y. Zheng, K. R. Choudhury, D. Bera, F. So, J. Xue, P. H. Holloway, *Nano Today* **2010**, *5*, 384.
[14] R. Meerheim, K. Walzer, G. He, M. Pfeiffer, K. Leo, *Proc. SPIE* **2006**, *6192*, 61920P.
[15] S.-J. Su, H. Sasabe, Y.-J. Pu, K. Nakayama, J. Kido, *Adv. Mater.* **2010**, *22*, 3311.
[16] H. Sasabe, T. Chiba, S.-J. Su, Y.-J. Pu, K. Nakayama, J. Kido, *Chem. Commun.* **2008**, 5821.
[17] Y.-J. Pu, M. Miyamoto, K. Nakayama, T. Oyama, M. Yokoyama, J. Kido, *Org. Electron.* **2009**, *10*, 228.
[18] K. Goushi, J. J. Brown, H. Sasabe, C. Adachi, *J. Appl. Phys.* **2004**, *95*, 7798.
[19] L. S. Liao, W. K. Slusarek, T. K. Hatwar, M. L. Ricks, D. L. Comfort, *Adv. Mater.* **2008**, *20*, 324.
[20] C. E. Small, S.-W. Tsang, J. Kido, S. K. So, F. So, *Adv. Funct. Mater.* **2012**, *22*, 3261.
[21] J. Kido, T. Matsumoto, *Appl. Phys. Lett.* **1998**, *73*, 2866.

[22] K. Walzer, B. Männing, M. Pfeiffer, K. Leo, *Chem. Rev.* **2007**, *107*, 1233.
[23] M. Pfeiffer, S. R. Forrest, K. Leo, M. E. Thompson, *Adv. Mater.* **2002**, *14*, 1633.
[24] A. Fukase, J. Kido, *Jpn. J. Appl. Phys.* **2002**, *41*, L334.
[25] D. Tanaka, H. Sasabe, Y.-J. Li, S.-J. Su, T. Takeda, J. Kido, *Jpn. J. Appl. Phys.* **2007**, *46*, L10.
[26] H. Sasabe, Y. Seino, M. Kimura, J. Kido, *Chem. Mater.* **2012**, *24*, 1404.
[27] H. Sasabe, N. Toyota, H. Nakanishi, T. Ishizaka, Y. J. Pu, J. Kido, *Adv. Mater.* **2012**, *24*, 3212.
[28] T. Matsushima, K. Goushi, C. Adachi, *Chem. Phys. Lett.* **2007**, *435*, 327.
[29] P. Santhanam, D. J. Gray, R. J. Ram, *Phys. Rev. Lett.* **2012**, *108*, 097403.
[30] D. Kim, L. Zhu, J.-L. Brédas, *Chem. Mater.* **2012**, *24*, 2604.
[31] Y. Noguchi, Y. Miyazaki, Y. Tanaka, N. Sato, Y. Nakayama, T. D. Schmidt, W. Brüttig, H. Ishii, *J. Appl. Phys.* **2012**, *111*, 114508.
[32] H. Sasabe, D. Tanaka, D. Yokoyama, T. Chiba, Y.-J. Pu, K. Nakayama, M. Yokoyama, J. Kido, *Adv. Funct. Mater.* **2011**, *21*, 336.
[33] H. Ishii, D. Tsunami, T. Suenaga, N. Sato, Y. Kimura, M. Niwano, *J. Surf. Sci. Soc. Jpn.* **2007**, *28*, 264.